

Symmetric Arsenic Dimers on the Si(100) Surface

R. I. G. Uhrberg, R. D. Bringans, R. Z. Bachrach, and John E. Northrup

Xerox Palo Alto Research Center, Palo Alto, California 94304

(Received 21 November 1985)

Deposition of arsenic on Si(100) results in a well-ordered, highly passivated, and stable surface. From a comparison between angle-resolved photoemission data and *ab initio* pseudopotential calculations we conclude that the observed 2×1 reconstruction is caused by the formation of symmetric As-As dimers on the surface. The calculated surface band dispersion for this model is in excellent agreement with experiment.

PACS numbers: 73.20.-r, 68.35.Bs, 79.60.Eq

A fundamental understanding of the electronic structure and bonding mechanisms involved in the reconstruction of semiconductor surfaces has been the objective of many experimental and theoretical studies. On the (100) surfaces of Si and Ge, dimer bonding between the atoms in the surface layer is considered to be the dominant reconstruction mechanism. Dimer formation alone leads to a 2×1 reconstruction. However, on Si and Ge(100), the surface symmetry is not simply 2×1 , but also contains regions of $p(2 \times 2)$ and $c(4 \times 2)$ symmetry.¹⁻⁴ The multiphase nature and disorder existing on Si(100)¹ makes a direct determination of the structure difficult.

One way to circumvent these problems is to create artificially a single-phase dimer surface which has a high degree of order. This allows us to separate the influence of dimer formation on the electronic structure from higher-order effects. The results we present here for Si(100)-As 2×1 show that As termination of the Si(100) surface does indeed yield a well-behaved dimer surface. Because surface-state dispersion is governed by the local atomic arrangement on the surface, we can use the band structure of the surface to determine structural information. In this paper we have carried out a detailed comparison between a theoretical prediction of the surface band structure of Si(100)-As 2×1 and the results of angle-resolved photoelectron spectroscopy which directly measures it. The comparison allows us to conclude that the As atoms form symmetric dimers on the Si(100) surface. Besides acting as a model for dimer formation in its purest form the Si(100)-As 2×1 surface is highly stable as a result of the passivating effect of the As and may have application to other studies.

In the symmetric As-As dimer model that we propose for the Si(100) surface, each As atom bonds to two Si atoms and to the other As atom of the dimer. This leaves all As atoms threefold coordinated with a doubly occupied lone-pair state. Because of the full coordination, the As atoms act as an efficient passivating layer, and the adsorption rate of additional As or contaminants was found to be highly reduced compared to the clean surface. The As-As dimer model is

structurally similar to the symmetric dimer models proposed initially for the clean Si(100) surface,⁵ but is very different chemically.

After a brief description of the experimental and theoretical techniques used, the remainder of the Letter discusses the model for Si(100)-As 2×1 in detail and makes a comparison of the experimentally determined surface-state dispersion with that predicted by the calculation.

Clean surfaces were obtained by repeated cycles of Ar⁺-ion sputtering (500 eV) and annealing (825 °C, 5 min) of a polished Si(100) crystal (*n*-type, $\rho \sim 0.5 \Omega \text{ cm}$). This cleaning procedure always resulted in a two-domain 2×1 LEED pattern. The Si(100) 2×1 surface showed strong emission from the dangling-bond-like surface state in normal emission and a dispersion which was found to be in good agreement with earlier studies.⁶⁻⁸ Arsenic was evaporated onto the Si(100) 2×1 surface in the form of As₄ molecules from a molecular-beam-epitaxy source. During deposition, the silicon sample was held at 400 °C to prevent adsorption of excess arsenic and to enable surface diffusion. The resulting Si(100)-As surface also showed a two-domain 2×1 LEED pattern, but with lower background intensity than for the clean surface. Annealing experiments confirmed that no excess arsenic was present on the surface after the exposure.

The angle-resolved photoemission measurements were performed by use of linearly polarized synchrotron radiation in the energy range 15.0–25.0 eV at the Stanford Synchrotron Radiation Laboratory. Two major azimuths were probed in the experiment and the orientation of these relative to the two 2×1 surface Brillouin zones (SBZ's) are shown in Fig. 1. Also indicated are the symmetry points of the two SBZ's.

Energy-minimization calculations were carried out for the class of structures consisting of dimerized As atoms on the Si(100) surface. These calculations employed the first-principles pseudopotential method⁹ and the local-density-functional formalism.¹⁰ The calculations were carried out in momentum space¹¹ and the Kohn-Sham¹⁰ equations were solved with a basis

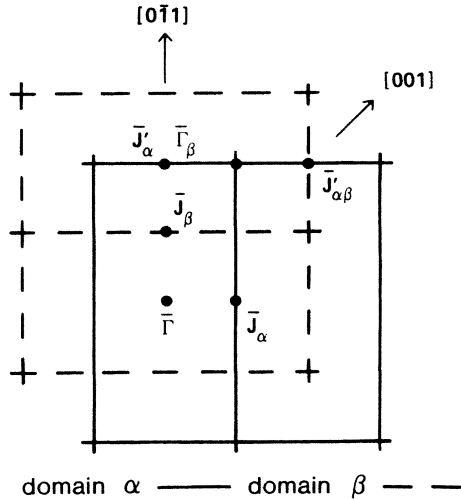


FIG. 1. Surface Brillouin zones for a two-domain 2×1 reconstruction on Si(100).

set consisting of plane waves with kinetic energy up to 7 Ry. A slab geometry containing eight layers of Si atoms and two layers of As atoms was used. Forces were calculated and used to determine the minimum-energy structure. Norm-conserving pseudopotentials were generated according to the method of Hamann, Schlüter, and Chiang¹² and the Ceperley-Alder¹³ correlation energy was used. This calculational technique has been applied previously to structural determinations of semiconductor surfaces.^{14, 15}

In the dimer geometries considered, each Si atom is fourfold coordinated and each As atom is threefold coordinated, as in the bulk of each material. The proposed minimum-energy structure is shown in Fig. 2. Each As atom is bonded to two Si atoms in the second layer and to the partner As atom in the dimer. The As-As dimer bond length is found to be 2.55 Å and the As-Si backbond length to be 2.44 Å. Buckling the dimer by 4°, while keeping the dimer and Si-As bond lengths constant, increases the total energy by 0.32 eV/surface atom. In addition, restoring forces leading back to the symmetric dimer structure are generated by such a buckling. The subsurface displacements induced by the dimer formation are also given in the figure. Although these displacements are large, they are explicable in terms of elastic considerations and are qualitatively similar to the subsurface displacements calculated in the symmetric dimer model⁵ for the clean Si(100) 2×1 surface with use of the Keating model. Thus the model that we propose for the Si(100)-As 2×1 surface contains symmetric rather than asymmetric dimers.

Angle-resolved photoemission measurements were carried out as a function of emission angle (θ_e) for the [001] and [011] azimuths of the Si(100)-As 2×1 surface. Spectra from the [001] azimuth were dominated

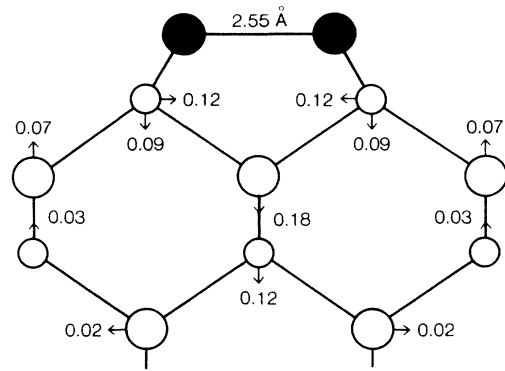


FIG. 2. Side view of the As-As dimer model of the Si(100)-As 2×1 surface with the As atoms shaded. The bond length between the As atoms and the subsurface displacements are indicated in angstroms.

by a single strong surface peak which we will refer to as $S_{\alpha\beta}$. Two strong surface state peaks, S_α and S_β , occur in the [011] direction. This is illustrated in Fig. 3 where spectra for symmetry points are shown. The positions of these peaks in energy and k_{\parallel} are presented in Fig. 4(a) for the full range of θ_e . Data for $h\nu = 21.2$ and 25.0 eV are plotted together in the left-hand part of the figure for the [001] azimuth and in the right-hand part for [011]. We have used a value of 0.95 eV for the separation of the top of the valence band, E_{VB} ,

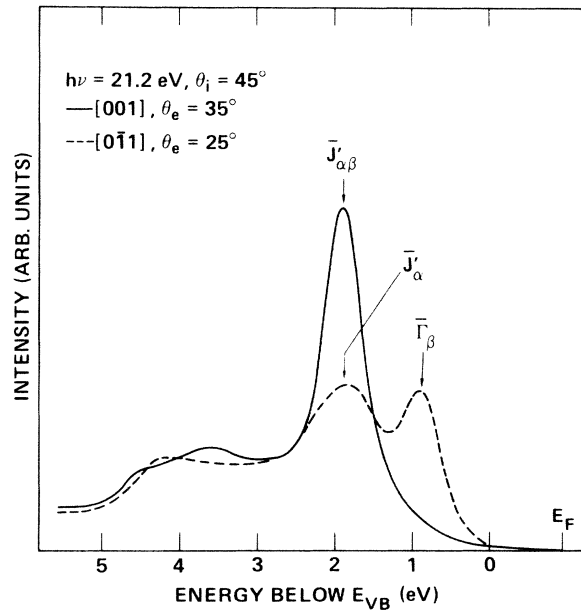


FIG. 3. Angle-resolved photoemission spectra obtained with linearly polarized synchrotron radiation. The spectra correspond to the points $J'_{\alpha\beta}$ and $(J'_\alpha, \Gamma_\beta)$ in the surface Brillouin zones.

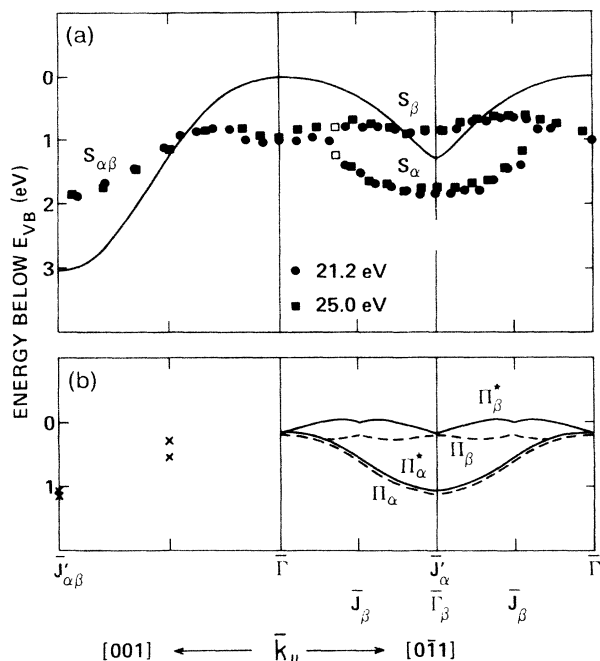


FIG. 4. (a) Experimental surface-state dispersion for Si(100)-As 2×1 in the [001] and [0 $\bar{1}1$] directions. The full curve shows the edge of the projected bulk band structure. Full (empty) symbols correspond to strong (weaker) spectral features. (b) Corresponding theoretical surface-state dispersions for the optimized symmetric As-As dimer model along the $\bar{\Gamma} \rightarrow \bar{J}'_{\alpha}$, $\bar{\Gamma} \rightarrow \bar{J}_{\beta}$, and $\bar{\Gamma} \rightarrow \bar{J}'_{\alpha\beta}$ lines.

from the Fermi energy, E_F . This value was determined by comparison of the energy position of the Si $2p_{3/2}$ peak for Si(100)-As with that of Si(100) 2×1 , for which we have used $E_F - E_{VB} = 0.46$ eV.¹⁶

The dispersions of the structures S_{α} , S_{β} , and $S_{\alpha\beta}$ can be seen in Fig. 4 to be independent of the photon energy. Additional measurements performed along the [0 $\bar{1}1$] direction for photon energies of 15.0 and 17.0 eV also gave the same dispersions. A small part of the dispersion for S_{β} and the major part of the $S_{\alpha\beta}$ dispersion lie within the bulk band gap. These observations, together with the fact that these structures are not present for the clean surface, lead us to interpret them as As-related surface states. Moreover, the surface-state assignment is supported by the periodicity of the dispersions. Along the [001] direction, for which we probe equivalent \bar{k}_{\parallel} lines for the two domains, we observe one surface band that is symmetric around $\bar{J}'_{\alpha\beta}$ as expected. In the [0 $\bar{1}1$] direction for which the lines $\bar{\Gamma} \rightarrow \bar{J}_{\beta}$ and $\bar{\Gamma} \rightarrow \bar{J}'_{\alpha}$ in the two 2×1 SBZ's are probed simultaneously, we observe two surface bands. All of the data are thus consistent with a single surface state per domain. An assignment of the two surface bands, S_{α} and S_{β} , to their proper domains can be made by examination of their periodicities. The dispersion of S_{α} is periodic around \bar{J}'_{α} and is

therefore associated with domain α . Structure S_{β} , which shows half the repeat length of S_{α} , is symmetric around \bar{J}_{β} and $\bar{\Gamma}_{\beta}$ and can therefore be assigned to domain β .

It is useful at this stage to compare the experimentally determined surface states with those calculated for our symmetric dimer model of the Si(100)-As 2×1 surface. As can be seen in Fig. 4 the overall agreement is excellent. The major feature of the electronic structure of the dimer model for Si(100)-As 2×1 is the occurrence of occupied π and π^* surface states which are nearly degenerate. In Fig. 4(b) we show these states by dashed (π) and solid (π^*) lines. In the [0 $\bar{1}1$] direction, where the photoemission simultaneously samples $\bar{\Gamma} \rightarrow \bar{J}$ and $\bar{\Gamma} \rightarrow \bar{J}'$, calculated dispersions for both directions are shown superimposed. The π and π^* bands are derived from symmetric (bonding) and antisymmetric (antibonding) combinations of the dangling hybrids on the As atoms. For a Si-Si dimer model of the clean Si(100) 2×1 surface only the π band is occupied. Replacement of the Si atoms in the dimer with As atoms adds two electrons per 2×1 unit cell and completely fills the π^* band. The splitting between the π and π^* states depends on the As-As dimer bond length d . Theory predicts $d = 2.55$ Å and a maximum π - π^* splitting of 0.23 eV. This is consistent with the fact that we do not resolve the two states in any of the spectra. If, however, the dimer bond length is reduced to 2.35 Å, the splitting increases to 0.47 eV and for $d = 2.15$ Å the splitting is 0.81 eV. Buckling of the dimers by 4°, for example, results in a separation of 0.95 eV between the two surface bands. These larger splittings, resulting from nonequilibrium geometries, are inconsistent with experiment. A large energy separation between the surface bands would give rise to two peaks in the [001] spectra. The single band observed in the experiment (small separation between π and π^* bands) supports a symmetric dimer model.

The agreement between calculation and experiment is very good in detail except for a rigid shift of 0.75 eV. This discrepancy is similar to those found in many previous calculations,¹⁵ and possibly arises because the self-energy corrections¹⁷ to the local-density-approximation eigenvalues may be different for surface and bulk states. The calculated bandwidth along the $\bar{\Gamma} \rightarrow \bar{J}'$ line is almost identical to the experimental value (0.9 eV compared to 0.8 eV). Along $\bar{\Gamma} \rightarrow \bar{J}$ the experiment shows a small upward dispersion also in good agreement with the calculation. For the nonsymmetry direction of the 2×1 SBZ the calculated initial-state energies are given at $\frac{1}{2}\bar{\Gamma}\bar{J}'_{\alpha\beta}$ and at $\bar{J}'_{\alpha\beta}$ and agree well with the experiment.

An interpretation of the experimental results in terms of a 2×1 dimer reconstruction is more straightforward for the Si(100)-As 2×1 surface than for the

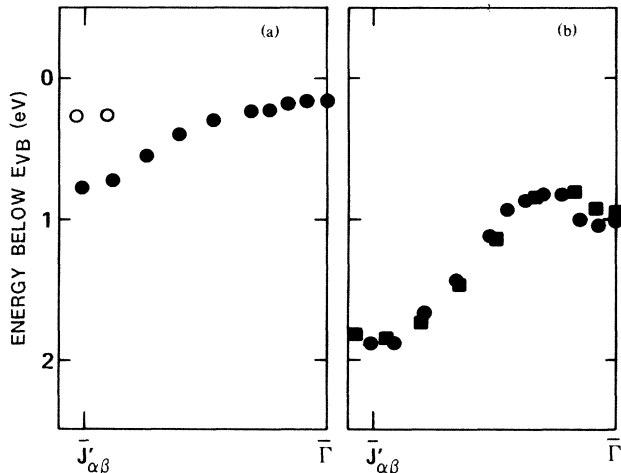


FIG. 5. Surface-state dispersions for (a) Si(100) 2×1 and (b) Si(100)-As 2×1 obtained with angle-resolved photoemission. Data taken with $h\nu = 21.2$ and 25.0 eV are shown by circles and squares, respectively. Full (empty) symbols correspond to strong (weaker) spectral features.

clean Si(100) 2×1 surface, since the model can account for all the surface states observed. This is not the case for clean Si(100) 2×1 where a second peak⁶⁻⁸ has been found close to \bar{J}' , along the [001] direction. The dispersion that we obtained for the clean Si(100) 2×1 surface is compared in Fig. 5 with the corresponding dispersion for Si(100)-As 2×1 . The upper feature for the clean surface cannot be explained in terms of a 2×1 dimer model alone and may be due either to disorder or to areas of higher-order reconstruction on the surface.

In summary, we have shown that the symmetric dimer model derived from energy-minimization calculations predicts surface-state dispersions for Si(100)-As 2×1 which agree well with those obtained with angle-resolved photoemission experiments.

We are pleased to acknowledge the skillful assistance of Lars Erik Swartz. Part of this work was per-

formed at the Stanford Synchrotron Radiation Laboratory, which is supported by the U. S. Department of Energy, Office of Basic Energy Sciences. The work of one of us (J.E.N.) was supported in part by the U. S. Office of Naval Research through Contract No. N00014-82-C-0244 and that of another of us (R.I.G.U.) was partially supported by the Swedish Natural Science Research Council.

¹R. M. Tromp, R. J. Hamers, and J. E. Demuth, Phys. Rev. Lett. **55**, 1303 (1985).

²J. J. Lander and J. Morrison, J. Chem. Phys. **37**, 729 (1962).

³T. D. Poppendieck, T. C. Ngoc, and M. B. Webb, Surf. Sci. **75**, 287 (1978).

⁴M. J. Cardillo and G. E. Becker, Phys. Rev. B **21**, 1497 (1980).

⁵J. A. Appelbaum and D. R. Hamann, Surf. Sci. **74**, 21 (1978).

⁶F. J. Himpsel and D. E. Eastman, J. Vac. Sci. Technol. **16**, 1297 (1979).

⁷R.I.G. Uhrberg, G. V. Hansson, J. M. Nicholls, and S. A. Flodström, Phys. Rev. B **24**, 4684 (1981).

⁸P. Koke, A. Goldmann, W. Mönch, G. Wolfgarten, and J. Pollman, Surf. Sci. **152/153**, 1001 (1985).

⁹M. L. Cohen, Phys. Scr. **T1**, 5 (1982).

¹⁰W. Kohn and L. J. Sham, Phys. Rev. **140**, A1135 (1965).

¹¹J. Ihm, A. Zunger, and M. L. Cohen, J. Phys. C **12**, 4409 (1979).

¹²D. R. Hamann, M. Schlüter, and C. Chiang, Phys. Rev. Lett. **43**, 1494 (1979).

¹³J. P. Perdew and A. Zunger, Phys. Rev. B **23**, 5048 (1981).

¹⁴M. T. Yin and M. L. Cohen, Phys. Rev. B **24**, 2303 (1981).

¹⁵J. E. Northrup and M. L. Cohen, Phys. Rev. B **27**, 6553 (1983).

¹⁶G. Hollinger and F. J. Himpsel, J. Vac. Sci. Technol. A **1**, 640 (1983).

¹⁷M. S. Hybertsen and S. G. Louie, Phys. Rev. Lett. **55**, 1418 (1985).